

Differential *MUC22* expression by epigenetic alterations in human lung squamous cell carcinoma and adenocarcinoma

SHUYE LIN¹, CUI MENG TIAN^{1,2}, JIANHUI LI³, BIN LIU¹, TENG MA¹, KEQIANG CHEN²,
WANGHUA GONG⁴, JI MING WANG² and JIAQIANG HUANG^{1,2}

¹Cancer Research Center, Beijing Chest Hospital, Capital Medical University/Beijing Tuberculosis and Thoracic Tumor Research Institute, Beijing 101149, P.R. China; ²Laboratory of Cancer Immunometabolism, Center for Cancer Research, National Cancer Institute at Frederick, Frederick, MD 21702, USA; ³Department of Pathology, Xuchang Central Hospital, Affiliated to Henan University of Science and Technology, Xuchang, Henan 461000, P.R. China; ⁴Basic Research Program, Leidos Biomedical Research, Inc., Frederick, MD 21702, USA

Received October 31, 2020; Accepted February 24, 2021

DOI: 10.3892/or.2021.8029

Abstract. Disruption in mucins (MUCs) is involved in cancer development and metastasis and is thus used as a biomarker. Non-small cell lung carcinoma (NSCLC) is characterized by heterogeneous genetic and epigenetic alterations. Lung adenocarcinoma (LUAD) and squamous cell carcinoma (LUSC) are the two primary subtypes of NSCLC that require different therapeutic interventions. Here, we report distinct expression and epigenetic alterations in mucin 22 (*MUC22*), a new MUC family member, in LUSC vs. LUAD. In lung cancer cell lines and tissues, *MUC22* was downregulated in LUSC (*MUC22^{Low}*) but upregulated in LUAD (*MUC22^{High}*) with co-expression of *MUC21*. The aberrant expression of *MUC22*

was inversely correlated with its promoter hypermethylation in LUSC and hypomethylation in LUAD cells and tissues, respectively. Decreased *MUC22* expression in NSCLC cell lines was restored upon treatment with epigenetic modifiers 5-aza-2'-deoxycytidine (5-Aza) or trichostatin A (TSA), accompanied by reduction in global protein level of histone deacetylase 1 (HDAC1) but increased enrichment of histone H3 lysine 9 acetylation (H3K9ac) specifically in the *MUC22* promoter in the SK-MES-1 cell line. *MUC22* knockdown increased the growth and motility of lung cancer cells and an immortalized human bronchial epithelial BEAS-2B cell line via NF- κ B activation. Clinically, *MUC22^{Low}* in LUSC and *MUC22^{High}* in LUAD were shown to be indicators of unfavorable overall survival for patients with early cancer stages. Our study reveals that changes in *MUC22* expression due to epigenetic alterations in NSCLC may have important biological significance and prognostic potential in LUSC when compared to LUAD. Thus, *MUC22* expression and epigenetic alterations may be used for molecular subtyping of NSCLC in precision medicine.

Correspondence to: Professor Jiaqiang Huang, Cancer Research Center, Beijing Chest Hospital, Capital Medical University/Beijing Tuberculosis and Thoracic Tumor Research Institute, 9 Ma Chang, Tongzhou, Beijing 101149, P.R. China
E-mail: huangjiaqiang@bjxkyy.cn

Abbreviations: 5-Aza, 5-aza-2'-deoxycytidine; TAA, tumor-associated antigen; BS, bisulfite sequencing; ChIP, chromatin immunoprecipitation; DEGs, differentially expressed genes; EGFR, epidermal growth factor receptor; EGFR-TKI, epidermal growth factor receptor-tyrosine kinase inhibitor; H3K9ac, histone H3 lysine 9 acetylation; HDAC1, histone deacetylase 1; HR, hazard ratio; CI, confidence interval; LUAD, lung adenocarcinoma; LUSC, lung squamous cell carcinoma; MSP, methylation specific-PCR; MSP-qPCR, methylation-specific real-time PCR; MUCs, mucins; *MUC22*, mucin 22; *MUC22^{High}*, high expression of mucin 22; *MUC22^{Low}*, low expression of mucin 22; NSCLC, non-small cell lung carcinoma; OS, overall survival; RT-PCR, reverse transcription-PCR; TSA, trichostatin A

Key words: mucin 22, non-small cell lung carcinoma, lung squamous cell carcinoma, lung adenocarcinoma, differential expression, epigenetic alterations, DNA methylation, histone acetylation, tumor heterogeneity, biomarker, molecular subtyping

Introduction

Non-small cell lung cancer (NSCLC) is the most common type of lung cancer and remains the leading cause of global cancer-related mortality and morbidity (1). As a highly diverse form of cancer, the heterogeneity of NSCLC is attributed to different histological origins as well as genomic and epigenetic abnormalities (2-4).

NSCLC is divided into two primary subtypes, adenocarcinoma (LUAD) and squamous cell carcinoma (LUSC), accounting for about 40 and 30% of all lung cancer cases, respectively (3,5). Anatomically, the tracheobronchial tree lined with respiratory epithelium is divided into central and peripheral compartments (6). LUAD and LUSC arise from different epithelial cell types with distinct genomic abnormalities and functional variability and thus require extremely different therapeutic strategies (2,3,5,7). For instance, adenocarcinomas predominantly originate from cells of

the peripheral airways secreting mucus and expressing biomarkers consistent with its distal bronchial origin, while squamous cell carcinomas mainly arise from the epithelium of the larger proximal airway (3,7). In contrast to the development of targeted therapies for lung adenocarcinoma, only a few oncogenic drivers have been identified in LUSC that limit the availability of targetable molecules for clinical trial (2,3,7). Also, it remains inconclusive whether these two tumor types stem from diverse cell types or from common precursor cells (3,5,8). Moreover, there is a substantial proportion of NSCLC lacking clear histological identity and biomarkers for subtyping (2,3,5,7,9). There are increasing reports showing acquired resistance to epidermal growth factor receptor-tyrosine kinase inhibitors (EGFR-TKIs) due to transformation of EGFR-mutant lung adenocarcinoma to squamous cell carcinoma (10,11). Therefore, more definitive markers are needed to distinguish the heterogeneity between LUSC and LUAD for precision treatment, especially for various resistance to targeted therapy.

Mucins (MUCs) are main components of the bronchiolar mucosal barrier, consisting of a family of high-molecular-weight glycoproteins expressed by specialized epithelial cells in secreted or membrane-bound forms (6,12). Among 21 mucins identified so far, most are expressed in the respiratory tract or lung parenchyma, including the secreted MUC2, MUC5AC, MUC5B, MUC7, MUC8 and MUC19 and membrane-bound MUC1, MUC3A, MUC4, MUC12, MUC13, MUC15, MUC16, MUC17, MUC20, MUC21 and MUC22 (6,12-15). Membrane-bound MUCs are present on epithelial cells serving as receptors and sensors to mediate signal transduction (12,13,16). Aberrant expression of MUCs is associated with the degree of lung cancer malignancy via multiple pathways (12,14,16). Therefore, MUCs are used as tumor-associated antigens (TAAs) and as immunotherapeutic targets for NSCLC (14,15,17).

Genetic and epigenetic profiling of lung cancer reveals differential expression of MUCs in diverse tumor microenvironments (14,18). In the present study, we examined the differential expression and epigenetic alterations of MUCs in LUSC and LUAD as potential tumor biomarkers. We found that *MUC22*, a new MUC family member, was decreased in the cells and tissues of LUSC (*MUC22^{Low}*) but increased in LUAD (*MUC22^{High}*) due to diverse epigenetic alterations. Distinct expression of *MUC22* in NSCLC was associated with varied outcome of patients. Our results suggest the potential of *MUC22* expression and its epigenetic alterations to distinguish NSCLC subtypes important for precision treatment.

Materials and methods

Patients and specimens. This study was approved by the Institutional Ethical Review Board for Human Investigation at Xuchang Central Hospital, Henan, China. Paired specimens including 24 LUSC and 24 LUAD tumors as well as tumor-adjacent tissues were obtained from 2002 to 2007 and stored at the Tissue Bank in accordance with the Standard Operating Procedures of the Ethics Committee of Xuchang Central Hospital (Table SI). The cohort included 33 males and 15 females (mean age, 60.38±12.19 years; range, 20-84 years). All patients signed informed consents.

Cell culture. Human NSCLC cell lines and human bronchial epithelial cell line BEAS-2B were obtained from ATCC (ATCC number: NCI-H1703, CRL-5889; NCI-H2170, CRL-5928; SK-MES-1, HTB-58; NCI-H226, CRL-5826; NCI-H1975, CRL-5908; NCI-H522, CRL-5810; NCI-H1395, CRL-5868; and HCC-827, CRL-2868). Cell lines were split to low density (30% confluence) and grown in 90% RPMI-1640 medium (Gibco; Thermo Fisher Scientific, Inc.) with 10% fetal bovine serum (FBS; Gibco; Thermo Fisher Scientific, Inc.). Before collection, cells were also treated with 5-aza-2'-deoxycytidine (5-Aza) (5 μM; Sigma-Aldrich; Merck KGaA) for 96 h with the growth medium being changed every 24 h, or TSA (5 μM, Sigma-Aldrich; Merck KGaA) for 24 h as previously described (19).

Knockdown of MUC22 using small interfering RNA (siRNA). Two siRNA oligonucleotides for *MUC22* (siMUC22-1 and -2) and RNAi Negative Control (siNC) were used in this study (Table SII). SiMUC22s were obtained from Beijing AUGCT Biotechnology Co. and siNC (siN0000002-1-5) were purchased from RiboBio, and were transfected into SK-MES-1, NCI-H522 and BEAS-2B cells using Lipofectamine 3000 according to the manufacturer's instructions (Invitrogen; Thermo Fisher Scientific, Inc.). After adequate knockdown efficiency was confirmed by RT-qPCR, the transfected cells were used for subsequent analyses.

RNA isolation, reverse transcription (RT) and polymerase chain reaction (PCR). RNA isolation, RT and PCR were performed as previously described (20,21). Cells were harvested for RNA isolation using RNeasy Mini Kit (Qiagen) and first-strand cDNA was synthesized with the Superscript First-Strand Synthesis System (Invitrogen; Thermo Fisher Scientific, Inc.). PCR was performed using primers listed in Table SII. qPCR was performed using 2X SYBR-Green-based qPCR reagent on ABI 7500 qPCR machine (Applied Biosystems). The relative expression level of each mRNA was normalized against β-actin using $2^{-\Delta\Delta C_q}$ method presented as 'relative expression (% of control)', or further compared to its own baseline control presented as 'normalized fold expression' (22).

DNA extraction, bisulfite modification, methylation-specific PCR (MSP-PCR) and bisulfite sequencing (BS). DNA extraction, bisulfite modification and MSP-PCR were performed as previously described (19,21). Genomic DNA was extracted from tissues using the QIAamp DNA mini Kit (Qiagen) followed by quantitative analysis using NanoDrop 1000 spectrophotometer (Thermo Fisher Scientific, Inc.). Bisulfite modification of DNA was performed using Zymo DNA Methylation Kit (Zymo Research). The positive and negative control were the Human Methylated & Non-methylated DNA Set (Zymo Research). MSP-qPCR was performed by using primer pairs specifically for either methylated or unmethylated sequences of the *MUC22* (Table SII). The relative level of methylation and unmethylation of *MUC22* promoter region was normalized to β-actin using the $2^{-\Delta\Delta C_q}$ method (19,22). MSP products were analyzed using a 2% agarose gel electrophoresis.

Western blot analysis. Total cell protein was prepared using RIPA Lysis Buffer (Beyotime Institute of Biotechnology). Protein was measured using a BCA protein Assay

Kit (CWBIO). Proteins were resolved by sodium dodecyl sulfate polyacrylamide gel electrophoresis (SDS-PAGE) and transferred onto PVDF membranes using a Bio-Rad Mini PROTEAN 3 system (Bio-Rad Laboratories, Inc.). The membranes were blocked with PBS containing 5% milk and 0.1% Tween-20 at room temperature for 1 h. The primary antibodies were as follows: β -actin (mouse monoclonal, dilution 1:10,000; A4551) was from Sigma-Aldrich; Merck KGaA. Lamin A (mouse monoclonal, dilution 1:1,000; sc-71481) was obtained from Santa Cruz Biotechnology, Inc. Anti-NF- κ B p65 (rabbit polyclonal, dilution 1:1,000; ab16502), anti-Histone H3 acetyl K9 (rabbit polyclonal, dilution 1:5,000, ab4441), anti-HDAC1 (rabbit polyclonal, dilution 1:5,000, ab109411) and anti-I κ B- α (rabbit polyclonal, dilution 1:5,000, ab32518) were purchased from Abcam. Horseradish peroxidase-conjugated anti-mouse (1:2,500 dilution) or anti-rabbit (1:2,500 dilution) secondary antibodies were purchased from Bioworld Technology, Inc. Immunoreactive bands were visualized by using the Amersham ECL Western Blotting Detection Kit (Cytiva) according to the manufacturer's instructions. β -actin served as a loading control (19,23).

Chromatin immunoprecipitation (ChIP). ChIP assay was performed by following EpiTech ChIPOneDay kit protocol (Qiagen) (19-21). SK-MES-1 cells with different treatments were fixed with 1% formaldehyde. Chromatin was prepared by sonication of cell lysate and pre-clearing with protein A beads. Aliquots of pre-cleared chromatin solution (named as 'IP fractions') were incubated with 2 μ g of specific rabbit anti-Histone H3 acetyl K9 or preimmune rabbit IgG on a rotation platform at 4°C overnight, and 1% of the IP fraction served as the 'Input control' for each ChIP assay. Protein A beads were added to precipitate the antibody-enriched protein-DNA complexes from the IP fractions. After washing, the immune complexes were subjected to reversal crosslink to release DNA fragments. Immunoprecipitated DNA fractions were purified by using a QIA quick purification kit (Qiagen) and analyzed by qPCR using 0.05% immunoprecipitated DNA as template.

Cell viability. SK-MES-1, NCI-H522 and BEAS-2B cells were seeded into 96-well plates at 2×10^3 cells/well, and cell viability was determined every day using 3-(4,5-dimethylthiazol-2-yl)-2,5-diphenyltetrazolium bromide (MTT) assay kit (Thermo Fisher Scientific, Inc.). The absorbance for MTT at 490 nm/570 nm wavelength was detected using a microplate reader (Thermo Multiskan MK3, Thermo Fisher Scientific Inc.) (23).

Migration assay. Transwell apparatus was inserted with an 8- μ m pore membrane (Corning Inc.). The upper chambers were seeded with serum-free medium containing 2×10^4 tumor cells in 200 μ l. The lower chambers were filled with 500 μ l of 10% FBS-RPMI-1640. After 24 h, the cells that migrated across the membrane were fixed and stained with 0.2% crystal violet (Beyotime Institute of Biotechnology). Images were then acquired using Leica microsystems (Leica DMi8 Inverted Microscope, GE) (23).

Statistical analysis. The data are expressed as the means \pm standard deviation (SD) of at least three independent experiments. The differences in *MUC22* expression and its

epigenetic alterations were analyzed by using the two-tailed Student's t-test or one-way analysis of variance (ANOVA) with Tukey's post hoc test. The relationship between *MUC22* and clinical pathologic characteristics was assessed by χ^2 tests. The difference of overall survival curve based on Kaplan-Meier plot was assessed for statistical significance with the Cramer-von Mises test using R package. All statistical analyses were performed using SPSS version 23.0 (IBM Corp.).

Results

Differential expression of *MUC22* in LUSC vs. LUAD. We first analyzed the RNA-Seq data of LUSC and LUAD in TCGA (The Cancer Genome Atlas) database (<https://www.cancer.gov/tcga>) (24) for the expression of membrane-bound mucins. After data consolidation, a total of 16,393 differentially expressed genes (DEGs) were identified, including 9,168 in LUSC (55.93%) and 7,225 in LUAD (44.07%). A total of 10,339 DEGs was upregulated (52.86% in LUSC and 47.14% in LUAD) and 6,054 DEGs were downregulated (61.17% in LUSC and 38.83% in LUAD) (Tables SIII and SIV). These results suggest a transcriptional heterogeneity within NSCLC.

Among DEGs graphically presented in a volcano plot according to the P-values and fold changes, we found differentially expressed mucin genes in NSCLC tissues (Fig. 1A). *MUC22* expression was significantly lower in LUSC (*MUC22^{Low}*) but higher in LUAD (*MUC22^{High}*) tissues (Fig. 1B) in association with lung adenocarcinoma-associated *MUC21*, whereas *MUCL1*, *MUCL4*, *MUCL13* and *MUCL20* were highly expressed in both LUAD and LUSC tissues, with consistently normal expression of *MUC12* (Table I). The distinct expression pattern of *MUC22* between LUSC and LUAD was further verified using GEPIA database data (<http://gepia.cancer-pku.cn/>) (25), showing *MUC22^{Low}* in LUSC (n=486) and *MUC22^{High}* in LUAD (n=483) as compared with normal tissues (Fig. 1C).

We then investigated the expression of *MUC22* in LUSC cell lines (NCI-H1703, NCI-H2170, SK-MES-1 and NCI-H226) and LUAD cell lines (NCI-H1975, NCI-H522, NCI-H1395 and HCC-827). As shown in Fig. 1D, *MUC22* mRNA expression was relatively lower in the LUSC cell lines but higher in the LUAD cell lines compared to the lung epithelial cell line BEAS-2B, except for the reversed expression pattern of *MUC22* in LUSC cell line NCI-H226 and LUAD cell line NCI-H1975, respectively. Paired specimens for further validation showed that the mRNA level of *MUC22* was significantly lower in LUSC, but enhanced in LUAD compared to matched adjacent normal lung tissues (Table II, Fig. 1E and F). Thus, *MUC22* is differentially expressed in NSCLC with distinction between LUSC and LUAD.

Epigenetic regulation of *MUC22* in human lung cancer cells and tissues. Given that epigenetic alterations, such as DNA methylation, can non-genetically modify gene expression resulting in functional disruption in cancer (19) or other disorders (26), we examined epigenetic contribution to the differential expression of *MUC22* in human lung cancer. MSP-qPCR was performed with lung cancer cell lines and tissues with primers covering the promoter region of *MUC22* (Fig. 2A). As shown in Fig. 2B, compared to BEAS-2B cells,

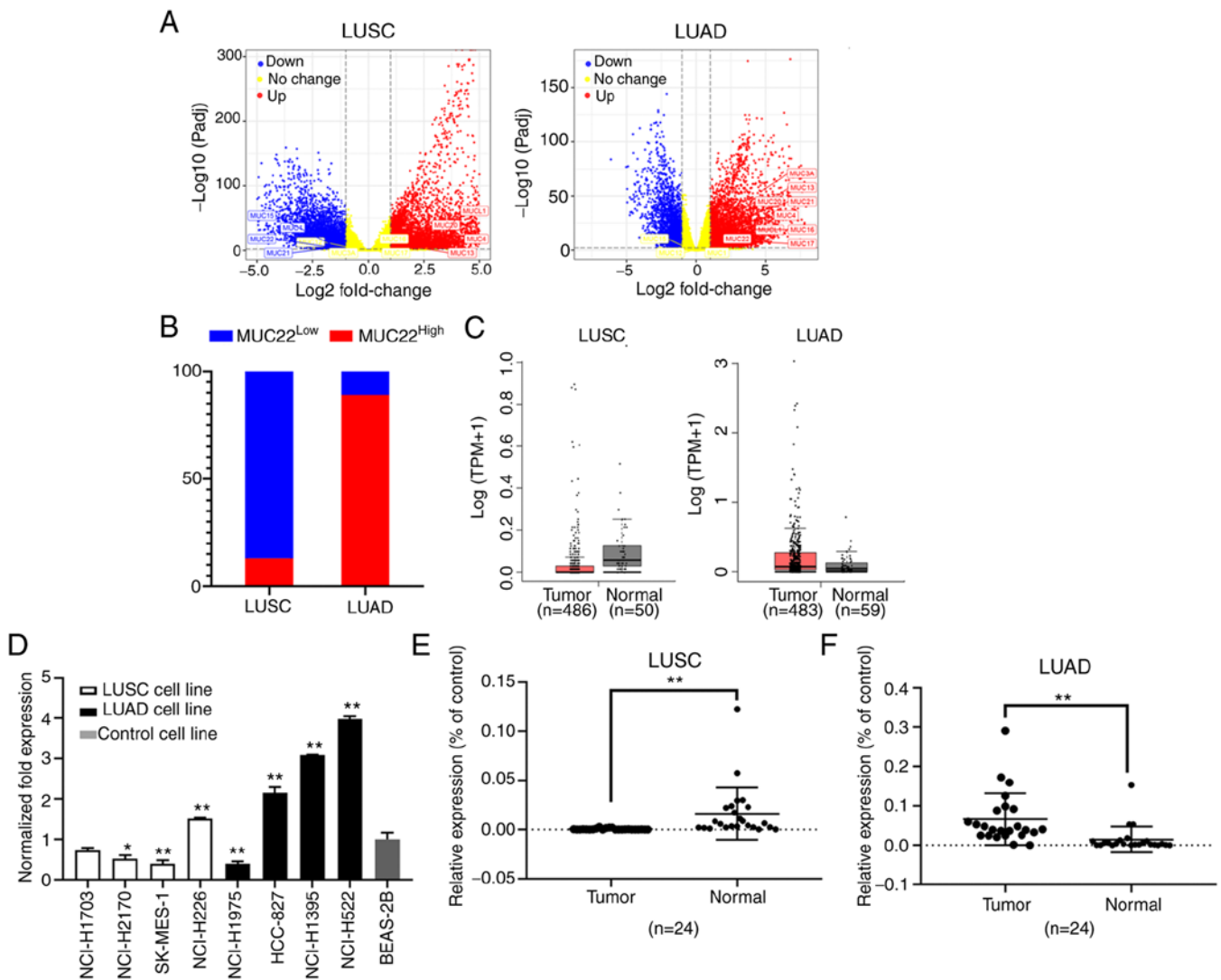


Figure 1. Differential expression of *MUC22* in human LUSC and LUAD cells and tissues. (A and B) Data were extracted from the TCGA RNA-Seq database (<https://www.cancer.gov/tcga>). Differentially expressed genes (DEGs) in TCGA-LUSC (Tumor=545, Normal=49) and TCGA-LUAD (Tumor=583, Normal=59) were analyzed by using iBio Tools v5.0. (A) Volcano plots showing DEGs ranked according to their statistical P-value for normalized \log_{10} transformed read counts of RNA-seq data (y-axis) and the absolute value of \log_2 fold change (x-axis) (data shown in Tables SIII and SIV). Colored spots represent significance upregulated (red) or downregulated (blue), or no change (yellow). Membrane-bound mucins are marked. (B) Shown is a 100% stacked bar chart showing differential expression of *MUC22* in LUSC (n=545) and LUAD (n=583) as compared with the normal controls. *MUC22*^{Low} or *MUC22*^{High} group was classified based on the default cutoff value used in the TCGA data portal (<https://www.cancer.gov/tcga>). (C) GEPIA portal analysis of TCGA RNA-sequencing results of *MUC22* mRNA in tumor tissues and normal lung tissues. Left: LUSC (Tumor=486, Normal=50); Right: LUAD (Tumor=483, Normal=58). The images were derived from GEPIA (<http://gepia.cancer-pku.cn/>). (D) RT-qPCR of *MUC22* mRNA in LUSC cell lines (NCI-H1703, NCI-H2170, SK-MES-1 and NCI-H226), LUAD cell lines (NCI-H1975, HCC-827, NCI-H1395 and NCI-H522) and an immortalized human bronchial epithelial BEAS-2B cell line. The relative expression of *MUC22* mRNA normalized with β -actin, and as fold of BEAS-2B is presented as the mean \pm SD. (E and F) RT-qPCR of *MUC22* mRNA in tumor tissues in comparison with paired normal control tissues of NSCLC patients. Detailed clinicopathologic parameters of patients are shown in Table S1. E, LUSC (n=24); F, LUAD (n=24). * $P < 0.05$ and ** $P < 0.01$, vs. relevant control (D, one-way ANOVA with Tukey's post hoc test; E and F, two-tailed Student's t-test). *MUC22*, mucin 22; LUSC, lung squamous cell carcinoma; LUAD, lung adenocarcinoma, NSCLC, non-small cell lung cancer.

the promoter region of *MUC22* was partially methylated in the LUSC cell lines, except NCI-H226 cells in which a more hypomethylated status of *MUC22* promoter was detected. Conversely, *MUC22* promoter was hypomethylated in LUAD cell lines, but heavily methylated in NCI-1975 cells. Further analysis showed that the promoter methylation of *MUC22* was associated reversely with its expression in the lung cancer cells (Fig. 2C). Consistently, the *MUC22* promoter was moderately or heavily methylated in 96% (23 of 24) of LUSC tissues, but unmethylated in 70% (16 of 23) of LUAD tissues ($P < 0.001$) associated with its expression in the tumors (100% *MUC22*^{Low} with methylation, $P < 0.001$)

(Figs. 2D and S1 and Table SV). These results suggested a closed correlation of *MUC22* promoter methylation with its expression.

We further investigated the epigenetic regulation of *MUC22* expression by treating LUSC cells with epigenetic modifiers, the DNA methyltransferase inhibitor 5-Aza or histone deacetylase inhibitor TSA. As shown in Fig. 2E, 5-Aza treatment markedly increased mRNA expression of *MUC22* in NCI-H1703, NCI-H2170 and SK-MES-1 cells, but not in NCI-H226 cells, whereas TSA significantly upregulated *MUC22* in NCI-H2170, SK-MES-1 and NCI-H226 cells, but not in NCI-H1703 cells. Moreover, TSA treatment of

Table I. Differential expression of membrane-bound mucins (*MUCs*) between LUSC and LUAD.

Type	Upregulated	Downregulated	Normal
LUSC	<i>UCL1^a, MUC4^a, MUC13^a, MUC20^a</i>	<i>MUC21^a, MUC22^b, MUC1^a, MUC15^a</i>	<i>MUC12, MUC3A, MUC16, MUC17</i>
LUAD	<i>MUC1^a, MUC4^a, MUC13^a, MUC20^a MUC21^a, MUC22^b, MUC3A^a, MUC16^a, MUC17^a</i>		<i>MUC12, MUC1, MUC15</i>

LUAD, lung adenocarcinoma; LUSC, lung squamous cell carcinoma. ^aP<0.05 and ^bP<0.01, vs. the control by t-test. Informative details are shown in the figure legend for Fig. 1A.

Table II. Association of *MUC22* expression with clinicopathologic parameters of the NSCLC patients (N=48).

Characteristics	No. of cases	<i>MUC22</i> ^{High} n (%)	<i>MUC22</i> ^{Low} n (%)	P-value
Total	48	27 (56.3)	21 (43.7)	
Sex				
Male	33	16 (48.5)	17 (51.5)	
Female	15	11 (73.3)	4 (26.7)	0.107
Age (years)				
≥60	25	13 (52.0)	12 (48.0)	
<60	23	14 (60.9)	9 (39.1)	0.539
Pathological type				
LUAD	24	21 (87.5)	3 (12.5)	
LUSC	24	6 (25.0)	18 (75.0)	1.3x10 ^{-5a}
Tumor invasive depth				
1	12	8 (66.7)	4 (33.3)	
2	31	17 (54.8)	14 (45.2)	0.481
3	5	2 (40.0)	3 (60.0)	0.309
Lymph node metastasis				
0	40	24 (60.0)	16 (40.0)	
1	8	3 (37.5)	5 (62.5)	0.242
Clinical stage				
I	3	2 (66.7)	1 (33.3)	
II	31	19 (61.3)	12 (38.7)	0.856
III	14	6 (42.9)	8 (57.1)	0.453

MUC22, mucin 22; NSCLC, non-small cell lung cancer; LUAD, lung adenocarcinoma; LUSC, lung squamous cell carcinoma. *MUC22* expression was analyzed by using RT-qPCR as shown in Fig. 2. ^aP<0.001 (χ^2 test).

SK-MES-1 cells resulted in reduction in the global protein level of histone deacetylase 1 (HDAC1) accompanied by a marked upregulation of acetylation of histone 3 at lysine 9 (H3K9ac) as analyzed by western blotting of whole cell extract (Fig. 2F). ChIP-qPCR analysis of genomic DNA immunoprecipitated with anti-H3K9ac antibody in SK-MES-1 cells showed that H3K9ac was significantly enriched in the *MUC22* promoter region upon the treatment (Fig. 2A and G). These results demonstrate that coordinated epigenetic modifications regulate *MUC22* expression in LUSC cells, in which epigenetic silent *MUC22* differentially responded to 5-Aza or TSA, suggesting heterogeneity of NSCLC cells subject to epigenetic regulation.

Knockdown of MUC22 promotes lung cancer cell growth and migration via NF- κ B activation. To explore the functional role of *MUC22* in lung cancer cells, siRNAs targeting *MUC22* (siMUC22-1 and 2) were transfected into SK-MES-1, NCI-H522 and BEAS-2B cells, and the knockdown efficiency was evaluated by RT-qPCR (Fig. 3A). As shown in Fig. 3B, knockdown of *MUC22* promoted the proliferation of both SK-MES-1 and NCI-H522 cell lines. Transwell migration assay showed significantly increased number of migrating SK-MES-1 and NCI-H522 cells after *MUC22* knockdown (Fig. 3C). These results suggest that *MUC22* inhibits the proliferation and migration of lung cancer cells. We further observed suppressive effect of *MUC22* on lung cell malignancy

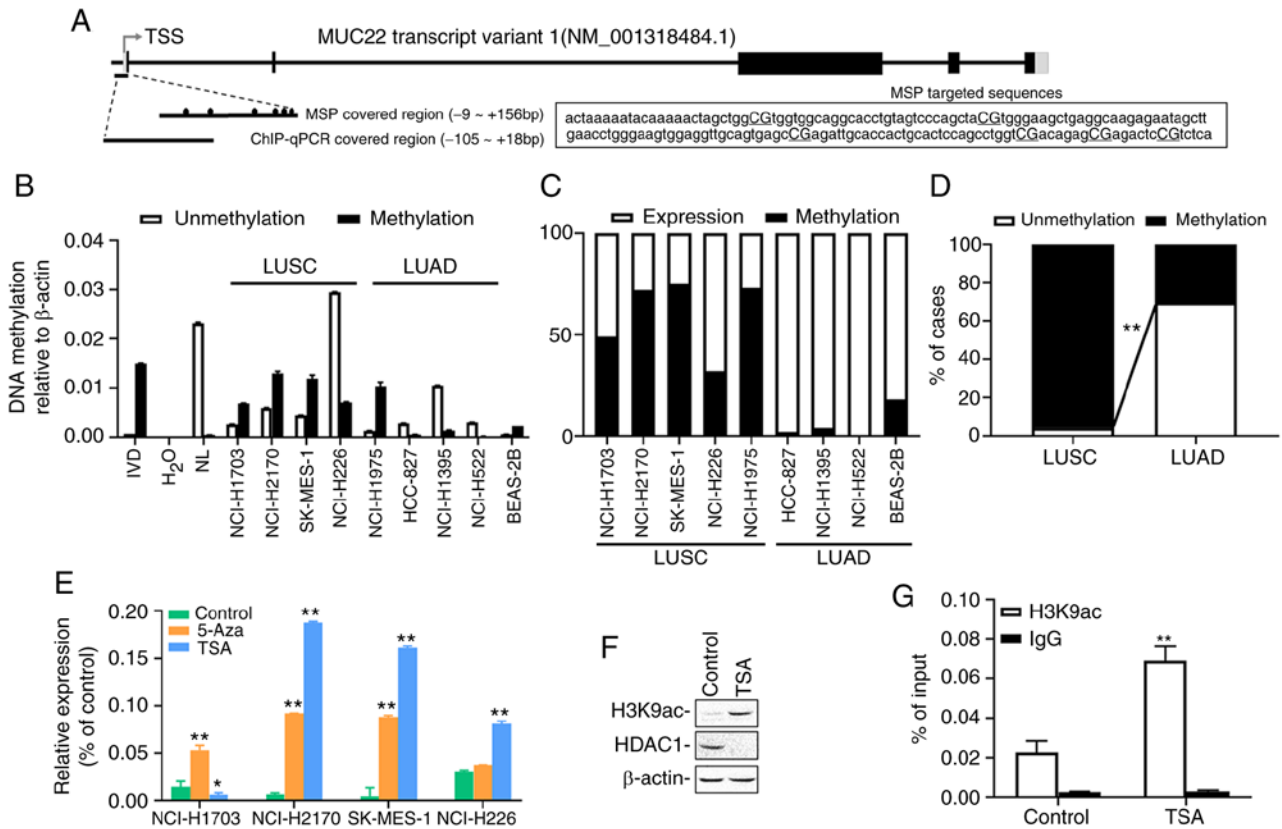


Figure 2. Epigenetic alterations of *MUC22* expression in LUSC and LUAD. (A) Schematic representation of *MUC22* transcript structure. The exons and introns are represented as boxes and lines. The regions targeted by primer pairs for methylation-specific PCR (MSP) and ChIP-PCR analysis are shown. Fragment sequences of *MUC22* for MSP are displayed with six CG sites capitalized and underlined. TSS, transcription start site. Black boxes, coding regions (CDS); gray boxes, untranslated regions (UTR); black ovals, CpG sites. (B) MS-qPCR analysis of *MUC22* methylation in LUSC cell lines (NCI-H1703, NCI-H2170, SK-MES-1 and NCI-H226), LUAD cell lines (NCI-H1975, HCC-827, NCI-H1395 and NCI-H522) and BEAS-2B cells. IVD, *in vitro* methylated DNA served as an MSP positive control; NL, normal blood lymphocyte DNA as negative control. (C) Comparative association between methylation and the expression of *MUC22* in LUSC and LUAD cell lines is visualized by 100% stacked bar graph. (D) The methylation frequency of *MUC22* promoter determined using MSP in LUSC (n=24) and LUAD (n=23) tissue samples. The frequency of methylation (M) and unmethylation (U) in the samples is presented as the percentage of cases. *MUC22* methylation in LUSC vs. LUAD. (E) RT-qPCR analysis of *MUC22* expression in cancer cells treated with epigenetic reagents, 5-aza-2'-deoxycytidine (5-Aza) or trichostatin A (TSA). The relative expression of *MUC22* mRNA normalized with β -actin is presented as the mean \pm SD. (F) Western blotting for H3K9ac and HDAC1 in SK-MES-1 cell lysates upon TSA treatment. (G) ChIP performed with SK-MES-1 cells after TSA treatment using antibody against H3K9ac or control IgG. Precipitated ChIP DNA fractions were analyzed by qPCR for the enrichment of H3K9ac in *MUC22* promoter region. Results are expressed as the percentage of input quantity. 5-Aza: 5 μ M, 96 h; TSA: 5 μ M, 24 h. *P<0.05 and **P<0.01, vs. the untreated control cells (D and G, two-tailed Student's t-test; E, one-way ANOVA with Tukey's post hoc test). *MUC22*, mucin 22; LUSC, lung squamous cell carcinoma; LUAD, lung adenocarcinoma.

in an immortalized bronchial epithelial cell line BEAS-2B, in which *MUC22* knockdown promoted cell growth and motility (Fig. 3A-C).

Nuclear factor (NF)- κ B as a key inflammatory regulator plays a critical role in the transformation of chronic inflammation towards carcinogenesis, which is preceded by aberrant expression of MUCs (12-14). We thus investigated the effect of *MUC22* on the NF- κ B pathway in lung cancer cells. As shown in Fig. 3D, transfection of SK-MES-1 cells with *MUC22* siRNAs resulted in a decrease in total I κ B- α , but an increase in the phosphorylated I κ B- α (p-I κ B- α) protein. However, there was no apparent changes in total p65 subunit of NF- κ B in whole cell extracts. Because both increased I κ B- α and reduced p-I κ B- α expression contribute to NF- κ B inactivation by trapping NF- κ B in the cytoplasm, the distribution of NF- κ B p65 subunit in lung cancer cells was examined, which showed a diminution of p65 in the cell cytoplasm with an augmentation in the nuclei upon siMUC22s transfection. Blockade of NF- κ B p65 subunit translocation indicates the ability of *MUC22* to inactivate NF- κ B. These results suggest

that epigenetic silencing of *MUC22* facilitates lung cancer cell growth and motility via NF- κ B activation.

Prognostic prediction value of distinct MUC22 in LUSC and LUAD. The potential prognostic prediction value of *MUC22* expression in LUSC (n=494) and LUAD (n=499) was assessed by Kaplan-Meier analysis of overall survival (OS) of *MUC22*^{Low} and *MUC22*^{High} lung cancer patients using the dataset available from the Human Protein Atlas (<http://www.proteinatlas.org>) (27) (Table SVI). As shown in Fig. 4A-E, Cramer-von Mises test analysis of the survival curves revealed that *MUC22*^{High} was significantly associated with favorable OS in LUSC patients but with worse OS in LUAD patients (Fig. 4A). Further analyses revealed the association of *MUC22*^{High} with more favorable outcome of LUSC patients at stages I and III cancer (Fig. 4B and D) but not at stages II and IV (Fig. 4C and E). By contrast, compared to *MUC22*^{Low}, *MUC22*^{High} LUAD patients had a significantly worse OS at stages I and II (Fig. 4B and C), but with a reversed outcome in patients with stage III cancer (Fig. 4D). The diverse association

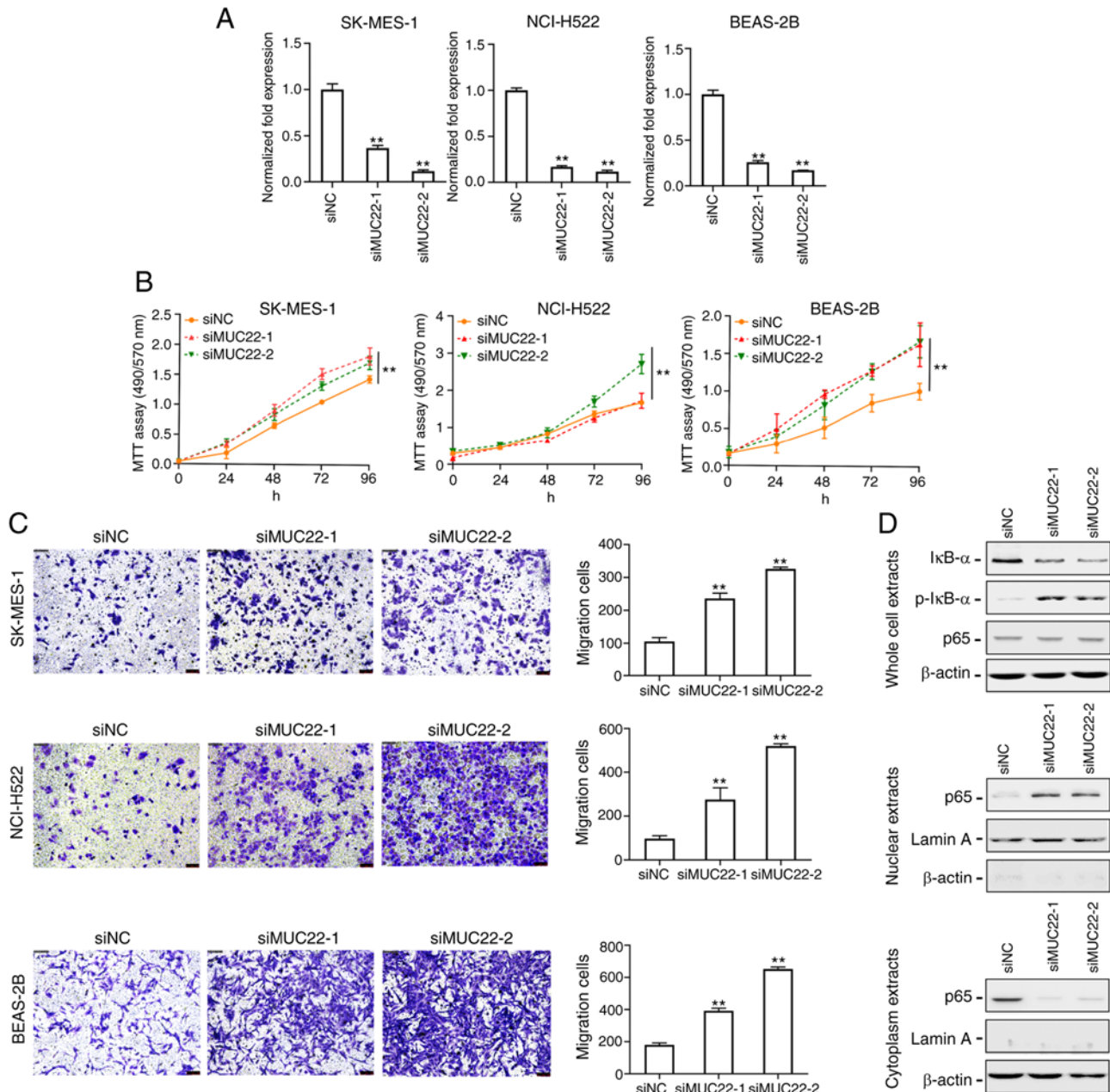


Figure 3. *MUC22* knockdown promotes lung cancer cell proliferation and migration via nuclear factor (NF)- κ B activation. (A) RT-qPCR analysis of the RNA interference efficiency. SK-MES-1, NCI-H522 and BEAS-2B cells were transfected with siRNA oligonucleotides (siMUC22-1 and -2) or with RNAi Negative Control (siNC). The expression of *MUC22* was then examined. (B) MTT assays showing the viability of SK-MES-1, NCI-H522 and BEAS-2B cells transfected with siMUC22s or siNC. Data are presented as the mean \pm SD. (C) The motility of SK-MES-1, NCI-H522 and BEAS-2B cells after transfection was assessed using Transwell assay shown with representative images (left panels) or quantification (right panels). (D) Western blot analysis of NF- κ B in SK-MES-1 cells upon *MUC22* knockdown. The protein levels of I κ B- α , p-I κ B- α and NF- κ B p65 subunit are shown in whole cell extracts (upper panel), nuclear extracts (middle panel) and cytoplasmic extracts (lower panel). β -actin serves as cytoplasmic, and Lamin A as nuclear protein loading controls, respectively. ** $P < 0.01$, vs. siNC. One-way ANOVA with Tukey's post hoc test was performed. *MUC22*, mucin 22; p-, phosphorylated.

of *MUC22* expression with patient survival with different stages of LUSC and LUAD reveals a complicated role of *MUC22* in tumor heterogeneity during cancer progression.

Discussion

In the present study, we revealed the biological significance and prognostic values of distinct expression and epigenetic alterations of mucin 22 (*MUC22*) in lung adenocarcinoma (LUAD) vs. squamous cell carcinoma (LUSC). Thus, *MUC22* may serve as a potential biomarker for subtyping non-small

cell lung cancer (NSCLC). Our research also provides evidence for mucins to contribute to the heterogeneous development of malignancy of lung cancer.

Mucins (MUCs) as a group of large glycoproteins expressed by various epithelial cells not only control the local environment but also contribute to cellular signal transduction in response to external stimuli (12,13,16). Abnormal MUC expression has been reported in various cancer types including lung cancer (12-15,18,19,28-30). In addition to several well-known mucins serving as tumor-associated antigens and cancer biomarkers particularly in adenocarcinomas (13,16,29,30), some

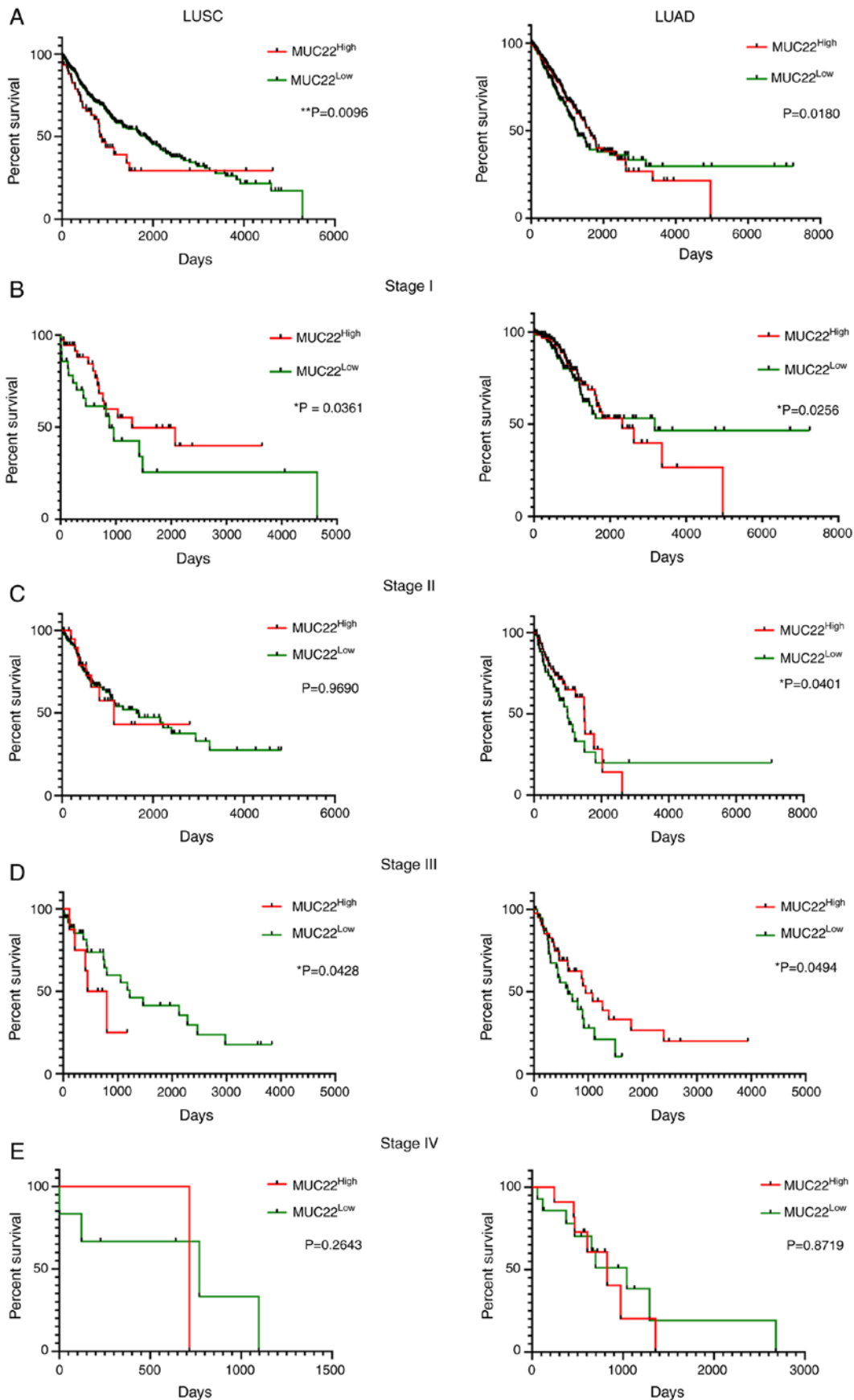


Figure 4. Prognostic prediction value of *MUC22* expression in LUSC and LUAD patients. RNA-sequencing data was obtained from the Human Protein Atlas (HPA, <https://www.proteinatlas.org>). Detailed clinicopathologic parameters are summarized in Table SVI. Kaplan-Meier survival analyses of overall survival of LUSC (left panels) and LUAD (right panels) patients with cancer at different stages. Patients with *MUC22*^{Low} or *MUC22*^{High} tumors at different stages were classified based on the cutoff value of 0.02, which is a default parameter also used in the Human Protein Atlas (sample sizes: LUSC: n=494; LUAD: n=499). Results are stratified in accordance with the expression patterns of *MUC22* in cancers of patients without staging (A), or with stage I (B), II (C), III (D), and IV (E). *P<0.05, **P<0.01, *MUC22*^{Low} vs. *MUC22*^{High} (Cramer-von Mises test). *MUC22*, mucin 22; LUSC, lung squamous cell carcinoma; LUAD, lung adenocarcinoma.

MUCs are preferentially distributed in the respiratory tract under normal conditions. Their disruption was reported in lung cancer and this has been used as biomarkers (13,16,30) as well as therapeutic targets (13,16,31-34). MUC22 is a novel membrane-bound mucin with previously unknown pathophysiological roles (35,36). We herein identified a distinct pattern of MUC22 expression, MUC22^{Low} in LUSC vs. MUC22^{High} in LUAD, in multiple lung cancer cell lines and tissues. We also found that MUC22 expression was significantly associated with MUC21 in both LUAD and LUSC tissues, differing from the higher expression of MUC11, MUC14, MUC13 and MUC20. Recent studies have shown aberrant expression of MUCs in LUAD including MUC1, MUC3A, MUC5B, MUC6, MUC7 and MUC21, in bronchial neoplasm (MUC4, MUC5AC, MUC5B, MUC6), or in small cell lung cancer (MUC1, MUC5AC, MUC3A, MUC6) (37-42). MUC21 is preferentially expressed in normal lung tissues particularly in the epithelia of bronchi and bronchioli (43). The divergence of MUC21 expression was shown in LUAD, but not in LUSC (39,40). MUC21 is known as an epiglycanin-like glycoprotein involved in the incohesive growth pattern in LUAD, and MUC21-expressing malignant bronchial epithelial cells may be the origin of LUADs (39,40,43). Since MUC22 was co-localized with MUC21 in a mucin gene cluster on chromosome 6p21.3 (36), co-expression of MUC22 with MUC21 may indicate a link between MUC21 and MUC22 in lung cancer progression contributing to lung cancer heterogeneity (14,16,31,44).

Epigenetic regulation of the expression of MUC1, MUC2, MUC4, MUC5AC and MUC17 has been reported under control by an interplay between DNA methylation and histone modifications in a variety of cancer cells (18,19,30,45-52). Our study demonstrated a more complicated epigenetic regulation of MUC22 in lung cancer. Although the differential expression of MUC22 was negatively correlated with MUC22 methylation status in multi-lung cancer cell lines and tissues and MUC22 silencing in LUSC is under the coordinated epigenetic modifications between DNA hypermethylation and histone deacetylation, increased MUC22 expression in LUAD was associated with the hypomethylation status in the promoter region. Promoter hypomethylation associated with mucin expression was also shown in several types of cancer cells and tissues, including lung cancer (45-48). Interestingly, instead of impacting gene transcription by methylation of CpG islands (CpGIs), we found there were six CpG sites in the MUC22 promoter region with their methylation status affecting MUC22 expression. Consistent with this, some MUCs, such as MUC1, MUC4, MUC5AC, MUC6 and MUC17, tend to have fewer CpG sites in their promoter regions or have distal CpG sites such as 'CpG island shore', or have a differentially methylated region (DMR), the methylation status of which is correlated with transcriptional regulation (18,19,31,46-51). Considering tissue-specific gene expression regulated by scattered or distal CpG sites, such as DMR, rather than CpG islands in the proximal promoter (53), the differential methylation status in the MUC22 promoter may determine the specificity of MUC22 expression during lung carcinogenesis. Therefore, the methylation status of the MUC22 promoter may serve as a noninvasive cancer biomarker to monitor the cell origin in lung carcinogenesis as well as therapy-resistant adenocarcinoma undergoing transformation to squamous cell carcinoma (10,11). Additionally, the pattern of epigenetic controlling of MUC22 expression

was opposite to what was predicted in LUSC NCI-H226 (MUC22^{High} with hypomethylation) and LUAD NCI-H1975 cells (MUC22^{Low} with hypermethylation), indicating that mucins contribute to inter- or intra-tumor heterogeneity in the context of epigenetic regulation (14,16,31,50).

The structural and functional link of MUC22 to lung cancer remains uncertain (12,14). We found that MUC22 knockdown promoted the growth and motility of lung cancer cells as well as an immortalized bronchial epithelial BEAS-2B cell line. The suppressive role of MUC22 in lung cancer cells was supported by the favorable prognostic prediction value of MUC22 in early stage LUSC, but not in LUAD. In support of our results, a recent report showed decreased MUC22 as one of three TP53-related prognostic signatures for LUSC (51). However, despite diverse effects of MUC22 expression on patient survival with different stages, the survival analysis showed that MUC22^{Low} in LUSC and MUC22^{High} in LUAD were associated with unfavorable outcome for patients at stage I but converted into protective factors at stage III. Since the prognosis in association with MUC22 expression in LUSC or LUAD became reversed in advanced lung cancer, a dynamic change in the role of MUC22 through the malignant process of LUSC or LUAD may be responsible for a functional heterogeneity in lung carcinogenesis (12,14,16). Therefore, it is important to delineate the precise molecular mechanisms underlying epigenetic regulation of MUC22 that contributes to phenotypic differences within NSCLC.

In conclusion, our research is the first to report the distinct expression and function of MUC22 in LUSC and LUAD. Epigenetic silencing of MUC22 may provide a molecular model for dissecting mucin-associated lung cancer heterogeneity, thus having clinical implication in distinguishing NSCLC subtypes for precision treatment.

Acknowledgements

Not applicable.

Funding

This study was funded by the Beijing Municipal Administration of Hospitals Incubating Program (PX2021063), the Intramural Research Funding Program from Beijing Tuberculosis and Thoracic Tumor Research Institute/Beijing Chest Hospital. CT, KC, WG, JH and JMW were also funded in part by federal funds from the National Cancer Institute, National Institutes of Health, under contract no. HHSN261200800001E and were supported in part by the Intramural Research Program of the NCI, CCR, LCIM, NIH.

Availability of data and materials

All data are publicly released from TCGA, GEPIA and CCLE databases and hyperlinks including citations have been included in the 'Results' section. Some of the data are also provided in the Electronic Supplementary Material.

Authors' contributions

Conceptualization of the research was conducted by SL, CT and JH. Methodology was designed by SL, CT, JL, BL,

TM, KC, and WG. Formal analysis and investigation were conducted by SL, CT, JMW, and JH. Writing of the original draft preparation was conducted by SL and JH; writing of the review and editing were performed by SL, JMW, and JH. Funding acquisition was provided by JMW and JH; resources were provided by JL and WG. Supervision was carried out by JH. All authors read and approved the manuscript and agree to be accountable for all aspects of the research in ensuring that the accuracy or integrity of any part of the work are appropriately investigated and resolved.

Ethics approval and consent to participate

This study was conducted with the approved of the Institutional Ethical Review Board for Human Investigation at Xuchang Central Hospital (Xuchang, Henan, China) and with informed consent from the patients.

Patient consent for publication

Not applicable.

Authors' information

Shuye Lin: ORCID: 0000-0002-4292-0302. Jiaqiang Huang: ORCID: 0000-0002-6610-8159.

Competing interests

The authors declare no competing interests.

References

- Bray F, Ferlay J, Soerjomataram I, Siegel RL, Torre LA and Jemal A: Global cancer statistics 2018: GLOBOCAN estimates of incidence and mortality worldwide for 36 cancers in 185 countries. *CA Cancer J Clin* 68: 394-424, 2018.
- Skoulidis F and Heymach JV: Co-occurring genomic alterations in non-small-cell lung cancer biology and therapy. *Nat Rev Cancer* 19: 495-509, 2019.
- Chen Z, Fillmore CM, Hammerman PS, Kim CF and Wong KK: Non-small-cell lung cancers: A heterogeneous set of diseases. *Nat Rev Cancer* 14: 535-546, 2014.
- Quintanal-Villalonga Á and Molina-Pinelo S: Epigenetics of lung cancer: A translational perspective. *Cell Oncol (Dordr)* 42: 739-756, 2019.
- Travis WD: Lung cancer pathology: Current concepts. *Clin Chest Med* 41: 67-85, 2020.
- Bustamante-Marin XM and Ostrowski LE: Cilia and mucociliary clearance. *Cold Spring Harb Perspect Biol* 9: a028241, 2017.
- Relli V, Trerotola M, Guerra E and Alberti S: Abandoning the notion of non-small cell lung cancer. *Trends Mol Med* 25: 585-594, 2019.
- Abbosh C, Birkbak NJ, Wilson GA, Jamal-Hanjani M, Constantin T, Salari R, Le Quesne J, Moore DA, Veeriah S, Rosenthal R, *et al*: Phylogenetic ctDNA analysis depicts early-stage lung cancer evolution. *Nature* 545: 446-451, 2017.
- Rotow J and Bivona TG: Understanding and targeting resistance mechanisms in NSCLC. *Nat Rev Cancer* 17: 637-658, 2017.
- Niederst MJ, Sequist LV, Poirier JT, Mermel CH, Lockerman EL, Garcia AR, Katayama R, Costa C, Ross KN, Moran T, *et al*: RB loss in resistant EGFR mutant lung adenocarcinomas that transform to small-cell lung cancer. *Nat Commun* 6: 6377, 2015.
- Roca E, Pozzari M, Vermi W, Tovazzi V, Baggi A, Amoroso V, Nonnis D, Intagliata S and Berruti A: Outcome of EGFR-mutated adenocarcinoma NSCLC patients with changed phenotype to squamous cell carcinoma after tyrosine kinase inhibitors: A pooled analysis with an additional case. *Lung Cancer* 127: 12-18, 2019.
- Dhanisha SS, Guruvayoorappan C, Drishya S and Abeesh P: Mucins: Structural diversity, biosynthesis, its role in pathogenesis and as possible therapeutic targets. *Crit Rev Oncol Hematol* 122: 98-122, 2018.
- Kufe DW: Mucins in cancer: Function, prognosis and therapy. *Nat Rev Cancer* 9: 874-885, 2009.
- Xu M, Wang DC, Wang X and Zhang Y: Correlation between mucin biology and tumor heterogeneity in lung cancer. *Semin Cell Dev Biol* 64: 73-78, 2017.
- Lucchetta M, da Piedade I, Mounir M, Vabistsevits M, Terkelsen T and Papaleo E: Distinct signatures of lung cancer types: Aberrant mucin O-glycosylation and compromised immune response. *BMC Cancer* 19: 824, 2019.
- Hollingsworth MA and Swanson BJ: Mucins in cancer: Protection and control of the cell surface. *Nat Rev Cancer* 4: 45-60, 2004.
- Jamal-Hanjani M, Wilson GA, McGranahan N, Birkbak NJ, Watkins TBK, Veeriah S, Shafi S, Johnson DH, Mitter R, Rosenthal R, *et al*: Tracking the evolution of non-small-cell lung cancer. *N Engl J Med* 376: 2109-2121, 2017.
- Yamada N, Kitamoto S, Yokoyama S, Hamada T, Goto M, Tsutsumida H, Higashi M and Yonezawa S: Epigenetic regulation of mucin genes in human cancers. *Clin Epigenetics* 2: 85-96, 2011.
- Lin S, Zhang Y, Hu Y, Yang B, Cui J, Huang J, Wang JM, Xing R and Lu Y: Epigenetic downregulation of MUC17 by *H. pylori* infection facilitates NF- κ B-mediated expression of CEACAM1-3S in human gastric cancer. *Gastric Cancer* 22: 941-954, 2019.
- Pan Y, Lin S, Xing R, Zhu M, Lin B, Cui J, Li W, Gao J, Shen L, Zhao Y, *et al*: Epigenetic upregulation of metallothionein 2A by diallyl trisulfide enhances chemosensitivity of human gastric cancer cells to docetaxel through attenuating NF- κ B activation. *Antioxid Redox Signal* 24: 839-854, 2016.
- Lin B, Zhou X, Lin S, Wang X, Zhang M, Cao B, Dong Y, Yang S, Wang JM, Guo M and Huang J: Epigenetic silencing of PRSS3 provides growth and metastasis advantage for human hepatocellular carcinoma. *J Mol Med (Berl)* 95: 1237-1249, 2017.
- Livak KJ and Schmittgen TD: Analysis of relative gene expression data using real-time quantitative PCR and the 2(-Delta Delta C(T)) method. *Methods* 25: 402-408, 2001.
- Lin S, Wang X, Pan Y, Tian R, Lin B, Jiang G, Chen K, He Y, Zhang L, Zhai W, *et al*: Transcription factor myeloid zinc-finger 1 suppresses human gastric carcinogenesis by interacting with metallothionein 2A. *Clin Cancer Res* 25: 1050-1062, 2019.
- Uhlen M, Zhang C, Lee S, Sjostedt E, Fagerberg L, Bidkhori G, Benfante R, Arif M, Liu Z, Edfors F, *et al*: A pathology atlas of the human cancer transcriptome. *Science* 357: eaan2507, 2017.
- Ghandi M, Huang FW, Jané-Valbuena J, Kryukov GV, Lo CC, McDonald ER III, Barretina J, Gelfand ET, Bielski CM, Li H, *et al*: Next-generation characterization of the cancer cell line encyclopedia. *Nature* 569: 503-508, 2019.
- Masser DR, Hadad N, Porter H, Stout MB, Unnikrishnan A, Stanford DR and Freeman WM: Analysis of DNA modifications in aging research. *Geroscience* 40: 11-29, 2018.
- Tang Z, Li C, Kang B, Gao G, Li C and Zhang Z: GEPIA: A web server for cancer and normal gene expression profiling and interactive analyses. *Nucleic Acids Res* 45: W98-W102, 2017.
- Jonckheere N and Van Seuningen I: Integrative analysis of the cancer genome atlas and cancer cell lines encyclopedia large-scale genomic databases: MUC4/MUC16/MUC20 signature is associated with poor survival in human carcinomas. *J Transl Med* 16: 259, 2018.
- Atanasova KR and Reznikov LR: Strategies for measuring airway mucus and mucins. *Respir Res* 20: 261, 2019.
- Yonezawa S, Higashi M, Yamada N, Yokoyama S, Kitamoto S, Kitajima S and Goto M: Mucins in human neoplasms: Clinical pathology, gene expression and diagnostic application. *Pathol Int* 61: 697-716, 2011.
- Nath S and Mukherjee P: MUC1: A multifaceted oncoprotein with a key role in cancer progression. *Trends Mol Med* 20: 332-342, 2014.
- Quoix E, Lena H, Losonczy G, Forget F, Chouaid C, Papai Z, Gervais R, Ottensmeier C, Szczesna A, Kazarnowicz A, *et al*: TG4010 immunotherapy and first-line chemotherapy for advanced non-small-cell lung cancer (TIME): Results from the phase 2b part of a randomised, double-blind, placebo-controlled, phase 2b/3 trial. *Lancet Oncol* 17: 212-223, 2016.

33. Hall PE, Ready N, Johnston A, Bomalaski JS, Venhaus RR, Sheaff M, Krug L and Szlosarek PW: Phase II study of arginine deprivation therapy with pegargiminase in patients with relapsed sensitive or refractory small cell lung cancer. *Clin Lung Cancer* 21: 527-533, 2020.
34. Taherali F, Varum F and Basit AW: A slippery slope: On the origin, role and physiology of mucus. *Adv Drug Deliv Rev* 124: 16-33, 2018.
35. Fini ME, Jeong S, Gong H, Martinez-Carrasco R, Laver NMV, Hijikata M, Keicho N and Argüeso P: Membrane-associated mucins of the ocular surface: New genes, new protein functions and new biological roles in human and mouse. *Prog Retin Eye Res* 75: 100777, 2020.
36. Hijikata M, Matsushita I, Tanaka G, Tsuchiya T, Ito H, Tokunaga K, Ohashi J, Homma S, Kobashi Y, Taguchi Y, *et al*: Molecular cloning of two novel mucin-like genes in the disease-susceptibility locus for diffuse panbronchiolitis. *Hum Genet* 129: 117-128, 2011.
37. Kim YK, Shin DH, Kim KB, Shin N, Park WY, Lee JH, Choi KU, Kim JY, Lee CH, Sol MY and Kim MH: MUC5AC and MUC5B enhance the characterization of mucinous adenocarcinomas of the lung and predict poor prognosis. *Histopathology* 67: 520-528, 2015.
38. Lee HK, Kwon MJ, Seo J, Kim JW, Hong M, Park HR, Min SK, Choe JY, Ra YJ, Jang SH, *et al*: Expression of mucins (MUC1, MUC2, MUC5AC and MUC6) in ALK-positive lung cancer: Comparison with EGFR-mutated lung cancer. *Pathol Res Pract* 215: 459-465, 2019.
39. Kai Y, Amaty VJ, Kushitani K, Kambara T, Suzuki R, Tsutani Y, Miyata Y, Okada M and Takeshima Y: Mucin 21 is a novel, negative immunohistochemical marker for epithelioid mesothelioma for its differentiation from lung adenocarcinoma. *Histopathology* 74: 545-554, 2019.
40. Yoshimoto T, Matsubara D, Soda M, Ueno T, Amano Y, Kihara A, Sakatani T, Nakano T, Shibano T, Endo S, *et al*: Mucin 21 is a key molecule involved in the incohesive growth pattern in lung adenocarcinoma. *Cancer Sci* 110: 3006-3011, 2019.
41. Lakshmanan I, Rachagani S, Hauke R, Krishn SR, Paknikar S, Seshacharyulu P, Karmakar S, Nimmakayala RK, Kaushik G, Johansson SL, *et al*: MUC5AC interactions with integrin β 4 enhances the migration of lung cancer cells through FAK signaling. *Oncogene* 35: 4112-4121, 2016.
42. Qu J, Yu H, Li F, Zhang C, Trad A, Brooks C, Zhang B, Gong T, Guo Z, Li Y, *et al*: Molecular basis of antibody binding to mucin glycopeptides in lung cancer. *Int J Oncol* 48: 587-594, 2016.
43. Itoh Y, Kamata-Sakurai M, Denda-Nagai K, Nagai S, Tsuiji M, Ishii-Schrade K, Okada K, Goto A, Fukayama M and Irimura T: Identification and expression of human epiglycanin/MUC21: A novel transmembrane mucin. *Glycobiology* 18: 74-83, 2008.
44. Wang DC, Wang W, Zhu B and Wang X: Lung cancer heterogeneity and new strategies for drug therapy. *Annu Rev Pharmacol Toxicol* 58: 531-546, 2018.
45. Yamada N, Nishida Y, Tsutsumida H, Hamada T, Goto M, Higashi M, Nomoto M and Yonezawa S: MUC1 expression is regulated by DNA methylation and histone H3 lysine 9 modification in cancer cells. *Cancer Res* 68: 2708-2716, 2008.
46. Yokoyama S, Higashi M, Kitamoto S, Oeldorf M, Knippschild U, Kornmann M, Maemura K, Kurahara H, Wiest E, Hamada T, *et al*: Aberrant methylation of MUC1 and MUC4 promoters are potential prognostic biomarkers for pancreatic ductal adenocarcinomas. *Oncotarget* 7: 42553-42565, 2016.
47. Okudaira K, Kakar S, Cun L, Choi E, Wu Decamillis R, Miura S, Wiest E, Matsuo K, Kitazono I, and Deng G: MUC2 gene promoter methylation in mucinous and non-mucinous colorectal cancer tissues. *Int J Oncol* 36: 765-775, 2010.
48. Yokoyama S, Higashi M, Tsutsumida H, Wakimoto J, Hamada T, Wiest E, Matsuo K, Kitazono I, Goto Y, Guo X, *et al*: TET1-mediated DNA hypomethylation regulates the expression of MUC4 in lung cancer. *Genes Cancer* 8: 517-527, 2017.
49. Kitamoto S, Yamada N, Yokoyama S, Houjou I, Higashi M, Goto M, Batra SK and Yonezawa S: DNA methylation and histone H3-K9 modifications contribute to MUC17 expression. *Glycobiology* 21: 247-256, 2011.
50. Vincent A, Perrais M, Desseyn JL, Aubert JP, Pigny P and Van Seuning I: Epigenetic regulation (DNA methylation, histone modifications) of the 11p15 mucin genes (MUC2, MUC5AC, MUC5B, MUC6) in epithelial cancer cells. *Oncogene* 26: 6566-6576, 2007.
51. Xu F, Lin H, He P, He L, Chen J, Lin L and Chen Y: A TP53-associated gene signature for prediction of prognosis and therapeutic responses in lung squamous cell carcinoma. *Oncimmunology* 9: 1731943, 2020.
52. Yamada N, Hamada T, Goto M, Tsutsumida H, Higashi M, Nomoto M and Yonezawa S: MUC2 expression is regulated by histone H3 modification and DNA methylation in pancreatic cancer. *Int J Cancer* 119: 1850-1857, 2006.
53. Lakshminarasimhan R and Liang G: The role of DNA methylation in cancer. *Adv Exp Med Biol* 945: 151-172, 2016.



This work is licensed under a Creative Commons Attribution-NonCommercial-NoDerivatives 4.0 International (CC BY-NC-ND 4.0) License.